Effects of oil on the curvature elastic properties of nonionic surfactant films: Thermodynamics of balanced microemulsions

Joakim Balogh,[1,*] Helena Kaper,[1,2] Ulf Olsson,[1] and Håkan Wennerström[1]
[1]*Physical Chemistry 1 Center for Chemistry and Chemical Engineering, Lund University, P.O. Box 125, SE-221 00 Lund, Sweden*
[2]*Physical Chemistry, CAU Kiel, Germany*
(Received 25 October 2005; published 11 April 2006)

The free energy of nonionic balanced microemulsions based on nonionic surfactants are analyzed using experimental data from (i) phase behavior, (ii) osmotic compressibility of the balanced microemulsion structure, which is obtained from small angle neutron scattering (SANS) experiments, and (iii) data on interfacial tensions obtained by T. Sottmann and R. Strey [J. Chem. Phys. **106** 8606 (1997)]. The balanced microemulsion, where the spontaneous curvature vanishes at equal volumes of water and oil, has a finite swelling with the solvent with a minimum surfactant volume fraction, Φ_S^*. At higher surfactant concentrations the balanced microemulsion phase having the surfactant volume fraction Φ_{S1} coexists with a lamellar phase of volume fraction Φ_{S2}. Under the constraint of $\Phi_W=\Phi_O$, where Φ_W and Φ_O are the water and oil volume fractions, respectively, the free energy density can be written as an expansion in the surfactant concentration. While the phase equilibria only depend on relative values of the expansion coefficients, absolute values can be obtained from compressibility and interfacial tension data. The osmotic compressibility of the surfactant film was measured by SANS through contrast matching water and oil. The phase behavior of nonionic surfactant-water-oil systems depends strongly on the chain length of the oil, when comparing a homologous series from octane to hexadecane using the same surfactant, here being pentaethylene oxide dodecyl ether ($C_{12}E_5$). The three concentrations Φ_S^*, Φ_{S1}, and Φ_{S2} increase markedly as the chain length of the oil is increased. However, from the analysis of the surface tension data it is concluded that there are no major changes in the bending rigidities as the oil is changed. The data are analyzed within the model free energy densities $G/V=a_3\Phi_S^3+a_5\Phi_S^5$ and $G/V=a\Phi_S^3(1+b\ln\Phi_S)$. We find that within experimental accuracy, the first of these models provides a quantitatively consistent description of the data. For the second model there is a larger discrepancy between observed and calculated values.

DOI: 10.1103/PhysRevE.73.041506 PACS number(s): 8380Qr

I. INTRODUCTION

Microemulsions are thermodynamically stable isotropic fluid mixtures of water and oil stabilized by a surfactant or a mixture of surfactants. While they are macroscopically homogeneous they have a structure on the 1–1000 nm length scale with water and oil domains separated by a surfactant film [1]. There is a large number of ways in which space can be divided into such domains, and surfactant-water-oil systems show a particularly rich phase behavior. These systems have also attracted a great deal of attention, due to the large number of practical applications related to such systems within the fields of enhanced oil recovery, food, pharmaceuticals, and cosmetics [2,3]. Microemulsions have been extensively characterized experimentally with respect to phase behavior, structure, and dynamic properties. However, there is a lack of fundamental understanding in the sense that the molecular mechanisms determining fundamental properties such as phase behavior, are not understood well enough to provide a predictive description. In microemulsion systems subtle effects determine the relative stability of different structures. In this paper we will take as an example the behavior of a series of ternary systems based on the surfactant dodecyl pentaethylene oxide ($C_{12}E_5$) with the oil being the normal alkanes octane, decane, dodecane, tetradecane, and hexadecane. Coupled to the modest variation in the length of the alkyl chain of the oil there are substantial quantitative changes in the phase equilibria. At balanced condition, where the bicontinuous microemulsion appears, the maximum swelling of the isotropic phase decreases by a factor of four in going from octane to hexadecane.

In order to provide a firm basis for an interpretation of this type of behavior we have used three types of experimentally determined properties to arrive at a quantitative description of the free energy. We have determined the maximum swelling of the microemulsions, confirming previous observations by Kahlweit and Strey and coworkers [4–7]. Additionally the precise location of the two-phase area microemulsion—lamellar phase has been measured as illustrated in Fig. 1. In independent experiments small angle neutron scattering (SANS) data has been collected. In the analysis we also make use of surface tension values carefully determined by Sottmann and Strey [5].

II. MICROEMULSION FREE ENERGY

Microemulsions and related phases have been successfully modeled as phases of fluid flexible surfaces, where one focuses on the curvature elasticity of the surfactant film [8–10]. The curvature free energy, G_c, of a given surface configuration is given by the surface integral $G_c=\int dA g_c$ of

*Electronic address: Joakim.Balogh@fkem1.lu.se

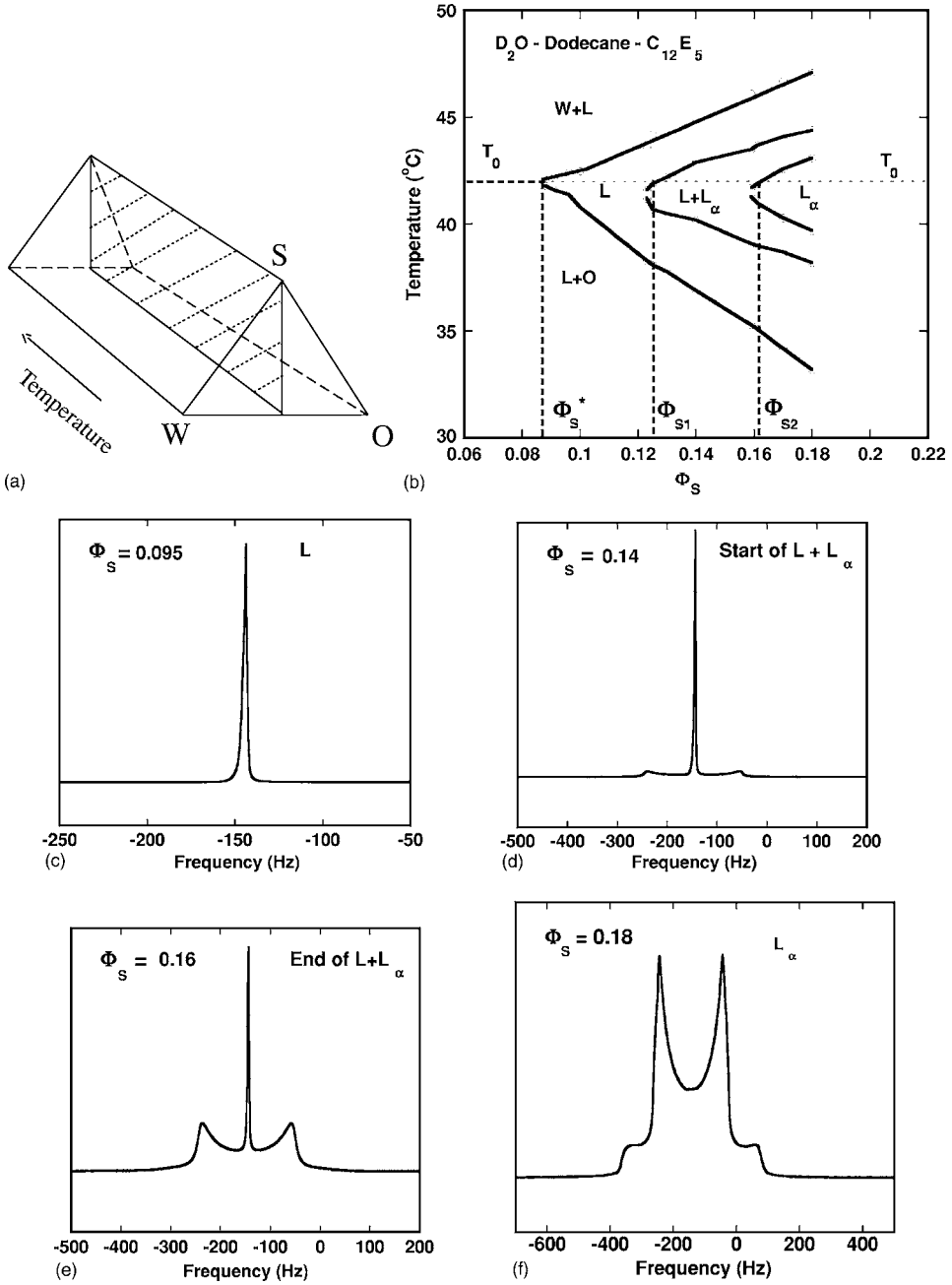

FIG. 1. The phase diagram of dodecane and the ^{2}H-NMR spectra for the microemulsion phase, the two phase area and the lamellar phase. An illustration of the phase prism of a ternary surfactant (S)-water (W)-oil (O) system is seen on the left side. The balance temperature T_0 and the concentrations Φ_S^*, Φ_{S1}, and Φ_{S2} can be seen in the phase diagram. The volume fraction surfactant is the total volume fraction of surfactant as is standard for phase diagrams. The observed values of Φ_S^*, Φ_{S1}, and Φ_{S2} can then be recalculated with Eqs. (18a) and (18b) to be the volume fraction of the film forming surfactant. These recalculated values are used through out the whole paper.

the curvature energy density, g_c. Within the harmonic approximation, g_c is conventionally written as [11]

$$g_c = 2\kappa(H - H_0)^2 + \bar{\kappa}K. \tag{1}$$

Here, H is the mean and K is the Gaussian curvature of the polar-apolar interface, and we use the convention that curvature towards oil is counted as positive. H_0 is the so called spontaneous curvature. The bending rigidity, κ, describes the resistance to conformations where H differs from H_0. The saddle splay constant, $\bar{\kappa}$ measures the stiffness relative to local saddle deformations of the film. Through the Gauss-Bonnet theorem it determines the global topological preference of the surfactant film. If $\bar{\kappa} < 0$, discrete microemulsion droplets are preferred, while if $\bar{\kappa} > 0$ the film prefers to adopt a locally saddle like shape, favoring a bicontinuous structure. The magnitudes of the two elastic constants are generally of the order of a few k_BT, and in practice κ is large enough so that the magnitude of H_0 plays a very important role in determining microemulsion structure and the phase behavior of the surfactant-water-oil system.

When the spontaneous curvature is zero the surfactant film has no preference to curve towards neither oil nor water and this is often referred to as the "balanced" state. It is found that a microemulsion can incorporate the maximum amount of solvent in the balanced state with equal volumes of water and oil. In this state the microemulsion with surfactant volume fraction Φ_S^* coexists with excess water and oil, forming a three-phase equilibrium. It adopts a bicontinuous structure where the midplane of the surfactant film forms a three dimensional simply connected surface of average zero mean curvature but with locally saddle like conformations

such that $\langle K \rangle < 0$. At higher surfactant concentrations, the balanced microemulsion is generically in equilibrium with a lamellar phase where the surfactant film is on average planar and the average values of both H and K are zero.

The thermodynamics and the relative stability of this spectacular phase pose a theoretical problem that has received considerable attention in the literature. Porte noticed that when $H_0=0$ the curvature energy resulting from Eq. (1) becomes independent of the length scale, and for a phase made of an infinite surfactant film this leads to a scaling law [12] for the total free energy density

$$G/V = a_3 \Phi_S^3, \tag{2}$$

where the coefficient a_3 can be either positive or negative. However, since this relation holds both for the lamellar phase and for the balanced microemulsion it is clear that a free energy expression having only Φ_S^3 term alone cannot describe the observed phase behavior with a finite swelling of the microemulsion and a microemulsion-to-lamellar transition on increasing the surfactant concentration. The phase having the lowest value of a_3 would globally be the most stable. Furthermore, depending on the sign of a_3, this phase would either swell infinitely with water and oil ($a_3>0$) or it would not swell at all ($a_3<0$). It is hence necessary to add an additional term to describe the observed phase behavior.

For lamellar phases Helfrich [13] has analyzed the entropic confinement of undulation modes as the concentration is increased and arrived an expression for the repulsive force. From his expression we arrive at the free energy by integration and the coefficient a_3 takes the positive value

$$a_3^{L_\alpha} = \frac{3\pi^2 (k_B T)^2}{128 \kappa l_S^3} (1-\Phi_s)^{-2}, \tag{3}$$

where l_S here is the surfactant monolayer thickness [14]. The factor $(1-\Phi_S)^{-2}$ is due to a correction for the finite thickness of the surfactant film. For bicontinuous microemulsions basically two approaches has been suggested for describing the free energy density. Based on the observation that the structural length scale in the bicontinuous microemulsion is inversely proportional to the surfactant volume fraction we have argued that at high volume fractions the local radii of curvatures are so large that it is necessary to go beyond the harmonic description of Eq. (1) for the bending energies [8]. This results in terms of higher order in Φ_S^* and

$$G/V = a_3 \Phi_S^3 + \sum_p a_p \Phi_S^p. \tag{4}$$

For a symmetrical film the first term in the sum is for $n=5$ and it has previously been shown that by including this term one obtains a qualitatively consistent description of microemulsions [10] and an quantitatively description of sponge phases [15,16]. However, for microemulsions the surfactant film is not symmetrical and we cannot exclude the possibility that also the $n=4$ term contributes. In a microscopic model the magnitude of coefficient a_4 is determined by a difference of the properties of the two layers on either side of the dividing surface. Placing the dividing surface at the polar-apolar interface yields for the $C_{12}E_5$ system two sublayers of approximately equal thickness, but with molecular differences. In this case the coefficient a_4 might be small due to cancellations, but it cannot be neglected *a priori*. In an alternative view [17–19] it has been argued that the physically important effect is the renormalization of the bending rigidity occurring at high dilutions. It is argued that this would introduce a logarithmic correction to Eq. (2) and

$$G/V = a \Phi_S^3 (1 + b \ln \Phi_S). \tag{5}$$

Although the two Eqs. (4) and (5) are clearly different both conceptually and mathematically it is far from straightforward to obtain data that clearly discriminates between the two descriptions. The latter approach has been used by more authors among them Gompper *et al.* [20]. The experimental data discussed in the following sections are aimed at determining the values of the coefficients in the models in such a way that we also obtain a critical test of the models.

III. INTERFACIAL TENSION

Sottmann and Strey have presented a systematic study of the water-oil (L1-L2) interfacial tension in nonionic microemulsions, using spinning drop measurements [5]. In these experiments the authors have explored the full temperature dependence and varied both the surfactant and the oil. Of particular interest here are the data for the $C_{12}E_5$ surfactant, where the oil has been varied from octane to tetradecane. These data show that the interfacial tension of a given system obeys the parabolic relation

$$\gamma = \mathcal{E}(T_0 - T)^2 + \gamma_0, \tag{6}$$

over a large temperature interval. Here ε is a constant and the value of the interfacial tension at $T=T_0$, denote γ_0, is numerically small compared to values obtained at temperatures a few degrees away from T_0. The plot of the surface tension data in Fig. 2 shows the striking effect that the data for the four different systems fall on the same line so that within the experimental accuracy ε takes the same value for the four systems.

At $T=T_0$ the interfacial tension takes a minimum value, γ_0, which is very low, in the order of 1 μN/m. In contrast to the constant value of ε, γ_0 varies by nearly an order of magnitude between the octane and the tetradecane system. How can we explain the similarities in ε and the differences in γ_0?

The interfacial tension, γ, reports on the free energy cost per unit area in forming a macroscopic planar film separating two phases. This film is locally the same as the film preexisting in the microemulsion phase and the interfacial tension can be written as

$$\gamma = g_i - g_{me}, \tag{7}$$

where g_i and g_{me} are the area free energy densities of the water-oil interface and the microemulsion phase, respectively. When analyzing the curvature energy of films that only bend into a spherical shape it is convenient to rewrite the curvature energy of Eq. (1) as

$$g_c = 2\kappa'(H - c_0)^2 - \bar{\kappa}(\Delta c)^2, \tag{1'}$$

where we have introduced the spherical bending constant

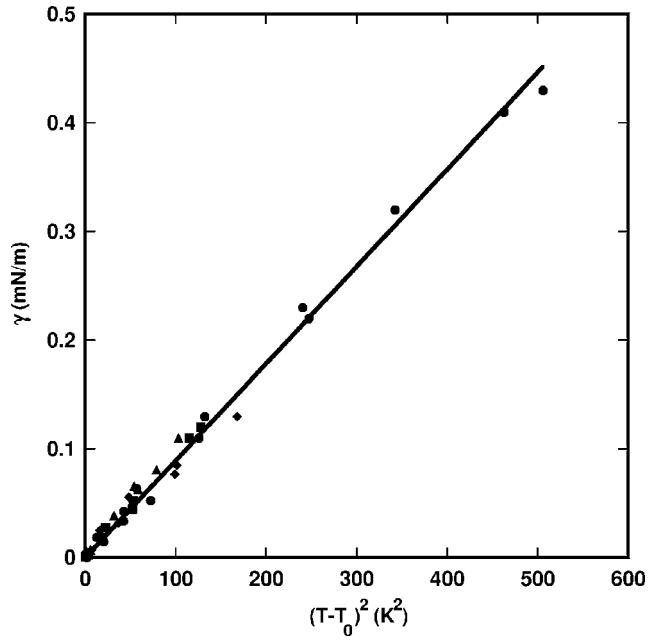

FIG. 2. Surface tension versus the squared temperature difference from T_0 is plotted for the different oils. The line is the fit to all the different oils. The oils are octane (circles), decane (squares), dodecane (diamonds), and tetradecane (triangles). Data taken from [5]. The offset γ_0 is numerically insignificant in the fitting.

$$\kappa' = \kappa + \frac{\bar{\kappa}}{2} \tag{8}$$

and the preferred spherical curvature c_0

$$c_0 = \frac{\kappa}{\kappa'} H_0. \tag{9}$$

The second term on the r.h.s of Eq. (1′) is determined by the difference in the principal curvatures and it vanishes for spherical systems. The curvature free energy density of flat films is

$$g_i = 2\kappa' c_0^2. \tag{10}$$

The parabolic dependence of γ on $(T_0 - T)$ in Eq. (6) can be understood as follows. The numerically significant γ values are obtained for droplet microemulsions. For these phases the free energy is the sum of a curvature and an entropy of mixing term. Neglecting the size polydispersity and assuming dilute conditions, and hence an ideal entropy of mixing, the microemulsion free energy is

$$G_{me} = N[8\pi\kappa'(1 - Rc_0)^2 + k_B T(\ln X_d - 1)], \tag{11}$$

where R is the radius of the droplet and X_d its' mole fraction.

The experiments by Sottmann and Strey where performed on samples where the microemulsion coexist with excess solvent, water, or oil. The surfactant remains in the microemulsion where the total film area is constant. As the temperature is varied there is a change in the radius R of the microemulsion droplets at the phase boundary. The droplets adjust to minimize the free energy of Eq. (11) under the constraint of constant film area. There is a balance between the curvature and the entropy terms and we find from Eq. (11) that at the optimum

$$Rc_0 = 1 + \frac{k_B T}{8\pi\kappa'} \ln X_d. \tag{12}$$

The second term on the r.h.s. is typically much smaller than one and the optimum R is dominantly determined by the minimization of the curvature energy. Combining Eqs. (7) and (10)–(12) we find that the surface tension is given by

$$\gamma = 2\kappa' c_0^2 \left[1 - \frac{k_B T}{8\pi\kappa'} \ln X_d \left(1 + \frac{k_B T}{8\pi\kappa'} \ln X_d \right)^{-1} \right]. \tag{13}$$

The main temperature variation of γ is according to this equation due to the temperature dependence of c_0. The temperature dependence of the spontaneous curvature H_0 has been extensively studied for $C_{12}E_5$ systems and around the balanced point there is a wide temperature range where the linear expansion remains valid and

$$c_0 = (\kappa/\kappa')H_0 = (\kappa/\kappa')\alpha(T_0 - T). \tag{14}$$

There is also a temperature dependence of the factor in the parenthesis in Eq. (13), but since the second term there is but a small correction term the parenthesis takes a nearly constant value. In addition to the effect of the factor T the mole fraction X_d also changes along the phase boundary. Using the fact that the total film area is conserved we find $\ln X_d \approx \ln X_S - \ln n_S^d$ where X_S is the, constant, mole fraction of surfactant relative to the solvent and n_S^d is the number of surfactant molecules per drop. The latter varies in the range 1×10^3–5×10^4 as the droplet size changes. Replacing n_S^d by the mean value 7×10^3 introduces a maximum error of ±2 in the expression $\ln n_S^d$. Sottmann and Strey used surfactant concentrations in the range of 1.5–5%(w/w). This corresponds to a geometric mean mole fraction of $X_S \approx 2\times10^{-3}$. Using these geometric mean values for X_S and n_S^d and Eqs. (13) and (14) we have

$$\gamma \approx 2.45 \frac{\kappa}{1 + \bar{\kappa}/2\kappa} \alpha^2 (T_0 - T)^2, \tag{15}$$

except close to $T = T_0$ where the interfacial tension takes a minimum value. Thus we have an approximate quadratic dependence of surface tension on $(T_0 - T)$ around the balanced point and

$$\varepsilon \approx 2.45\kappa\alpha^2/[1 + \bar{\kappa}/(2\kappa)]. \tag{16}$$

The data in Fig. 2 implies that the product $\kappa\alpha^2/[1+\bar{\kappa}/(2\kappa)]$ is independent of the oil chain length. From previous studies [21], we have that $\alpha = 5\times10^6$ m^{-1} K^{-1} and it is within experimental accuracy independent of the oil chain length. From the slope of the line 8.9×10^{-7} Jm^{-2} K^{-2} in Fig. 2, we obtain $\kappa/[1+\bar{\kappa}/(2\kappa)] = 1.4\times10^{-20}$ J from Eq. (16) for all four systems. This value is consistent with the value $\kappa/[1+\bar{\kappa}/(2\kappa)] = 1.6\pm0.4\times10^{-20}$ J [16], obtained previously for the decane system. From this we conclude that the marked difference in phase behavior between the four systems is not due to a difference in the bending rigidity of the film. The systems differ only by the length of the alkyl chain in the oil in the medium on one

TABLE I. The minimum surface tension, γ_0 from [5] is here, data used to calculate $G/V/(\Phi_S^*)/c_1$. Here we used $l_S=15$ Å.

Table I	Octane	Decane	Dodecane	Tetradecane	Hexadecane
γ_0/Jm^{-3}	5×10^{-7}	9×10^{-7}	2.3×10^{-6}	4.7×10^{6}	
$G/V/(\Phi_S^*)\mathrm{Jm}^{-3}$	−12.1	−34.2	−119	−228	

side of the film. It is thus not surprising the bending rigidity is within experimental accuracy the same in the four systems, as also suggested earlier [5,21,22].

The systems do differ in the values of the low surface tension observed in the three-phase triangle. From Eq. (7) it is seen that the surface tension in this case, $H_0=0$, is solely due to the free energy cost of transforming the complex topology of the film in the bulk into a planar layer, which represents the implicit standard state for the free energy expansions in Eqs. (2)–(5). Under the assumption that the actual area of the film at the interface equals the macroscopic projected area of that interface, we have that the surface tension equals minus the free energy per film area at maximum swelling so that

$$G/V = -\gamma_0\Phi_S^*/l_S, \tag{17}$$

and we have an absolute estimate of the free energy at a specific concentration. The observation that γ_0, see Table I, differs greatly between the different systems is then qualitatively consistent with the fact that the maximum swelling Φ^* also varies substantially. From Eq. (17) we obtained a value for the free energy density G/V for a particular concentration of the four systems. In order to get a more detailed characterization of the free energy, we have performed small angle neutron scattering studies as well as careful determinations of phase boundaries.

IV. MATERIALS AND METHODS

A. Materials

Hexadecane (99%+), tetradecane (99%+), dodecane (99%+), decane (99%+), and octane (98%+) were purchased from Sigma-Aldrich Chemie (Germany). The heavy water D_2O (99.8% isotopic purity) was purchased from Dr Glaser AG (Switzerland). The deuterated solvents, C_8D_{18}, (D99%) $C_{10}D_{22}$, (D99%) $C_{12}D_{26}$, (D98%) $C_{14}D_{30}$, (D98%), and $C_{16}D_{34}$ (D98%) were purchased from Cambridge Isotope Laboratories (Cambridge, MA). The nonionic surfactant $CH_3(CH_2)_{11}(OCH_2CH_2)_5OH$ ($C_{12}E_5$) was purchased from Nikko Chemicals (Japan). The α-deuterated nonionic surfactant $CH_3(CH_2)_{10}CD_2(OCH_2CH_2)_5OH$ used for the NMR experiments was synthesized by Synthelec (Lund, Sweden). These chemicals were used without further purification.

B. Phase diagram determination

The samples were weighed into tubes sealed with screw caps. The samples were mixed with a vortex mixer at 5 °C above the upper stability limit of the microemulsion phase and then mixed while cooling to the microemulsion phase and kept there before any measurement.

The samples were studied in a thermostated water bath. Phase-boundary temperatures were determined by visual inspection, including the use of crossed polarizers, especially by going from the clear phase to a turbid phase. The kinetics of the macroscopic phase separation of the microemulsion and excess oil phase are slow [23]. The boundaries were determined both from higher temperatures and from lower temperatures. We looked both at the phase separation and the solubilization. NMR was used to complement the use of polarizers to determine phase composition as illustrated in Fig. 1. The lamellar phase is anisotropic and thus birefringent while the isotropic microemulsions do not show any birefringence at rest.

C. ^{2}H-NMR

Some samples were investigated with deuterium NMR where the deuterium was present in the D_2O and, as a result of chemical exchange, in the hydroxyl group of the surfactant. These experiments were mainly used to identify the microemulsion-lamellar phase equilibrium at the balance temperature T_0. ^{2}H is a spin $I=1$ nucleus carrying an electric quadrupolar moment [24]. In the anisotropic environment of the molecules, as in the lamellar phase, the quadrupolar interaction is not completely averaged to zero, resulting in line splitting, a so called quadrupolar splitting, with the frequency separation $\Delta\nu_Q$. In the isotropic microemulsion phase, on the other hand, the quadrupolar interaction becomes completely averaged to zero and the NMR spectrum consists of singlet. In the microemulsion-lamellar two-phase region the spectrum consists of a superposition of a singlet and doublet. The relative areas under the peaks report on the relative amounts of the two coexisting phases (here, the water concentration). The NMR samples were prepared by transferring the samples at the upper microemulsion phase into 5 mm NMR tubes and then immediately flame sealing them, to avoid solvent evaporation. The measurements were performed on a Bruker DMX 200 advance NMR spectrometer with a 4.6 T magnet. The temperature of the sample was maintained using an airflow system to an accuracy of ±0.1 °C.

D. SANS

Small Angle Neutron Scattering (SANS) experiments were carried out on SANS1 at Paul Scherrer Institut (PSI) in Villigen Switzerland [25]. The q range covered was $0.0020 < q < 0.4$ Å^{-1}. The resolution is influenced by various factors. The main and limiting contribution is the wavelength

spread of around 10%. The mean neutron wavelength was 10 Å. Other factors like beam collimation effective pixel size, radial averaging, etc. were adjusted not to limit the resolution. Temperature was controlled with a thermo-stated bath prior to insertion in the thermo-stated sample holder.

Water was used to determine the detector sensitivity and absolute scale calibration. This was done at 2 m with 6 m collimation with sufficiently good statistics and the other distances were measured for a shorter time so that calibration factors for both 6 m detector distance and 6 m collimation and for 18 m detector distance and 18 m collimation, could be calculated. The individual cells of the 128×128 pixel two-dimensional (2D) detector were already found to be uniform. The spurious scattering around the beam stop and on the outer rim of the detector was masked. The raw data were masked, averaged and normalized using the BerSANS program at PSI [26]. The scattering of empty cell and empty beam was subtracted from the water and sample measurements with the transmission taken into account. The overlapping data was used to fudge the three curves into one. The same scaling parameters were used for all oils, 0.9 for 6 m and 0.81 for 18 m. The coherent scattering component of the differential cross section per unit volume is denoted $I(q)$.

There are several factors influencing the accuracy of this number. First of all the temperature is not accurately fixed and there is a significant temperature gradient across the scattering volume where the temperature may vary by several tenths of degrees. While the main part of the sample cell is in reasonable thermal contact with a metal heating block, the front and back windows in the block, required for the passing of the neutron beam, are colder areas. Hence, one expects approximately parabolic temperature profiles both in the vertical and horizontal directions around the window center where the temperature is expected to take a minimum. The larger the temperature difference is from room temperature, the larger is the expected temperature gradient. By using a thermocouple, we measured the temperature at different positions in the vertical direction. When thermostating the sample to approximately 50 °C (hexadecane system), the temperature varied by approximately 0.5 °C across the scattering volume.

E. Correcting for the surfactant solubility in the oil

The surfactant is partly soluble in the oil and that part does not contribute to the film forming. When doing our calculations we used only the surfactants that are not in the oil domain. The film forming surfactant can be calculated through

$$\Phi_S = \Phi_{STotal} - \Phi_O^* \Phi_{SinOil}, \tag{18a}$$

where for $\Phi_W = \Phi_O$

$$\Phi_O = \frac{1 - \Phi_S}{2}, \tag{18b}$$

and Φ_{SinOil} is the solubility of surfactant in oil taken from Ref. [27].

V. SMALL ANGLE NEUTRON SCATTERING AND OSMOTIC COMPRESSIBILITY

Small angle neutron scattering, SANS, has been used extensively to characterize the structure of microemulsions. One conclusive result from such measurements is the confirmation of the $1/\Phi_S$ scaling law for the structure in the bicontinuous microemulsion. For each of the five systems we have performed SANS measurements for two concentrations under conditions of surfactant film contrast. In spite of the fact that the concentrations are clearly different for the different systems the data at high and medium q values fall on one single curve for all samples, when the proper scaling is made as shown in Fig. 3. The observed consistency of the scattering intensities at these q values shows that the local structure is the same for all systems after correcting for the difference in length scale.

As the water and oil are contrast matched the microemulsion can be considered as an effectively binary system, assuming that the microstructure is symmetric with respect to the exchange of water and oil domains. In this case, the forward scattering intensity $I(0)$ is related to the thermodynamic quantity denoted osmotic compressibility. This in turn is simply related to the second derivative of the free energy density and

$$\left(\frac{\partial^2 (G/V)}{\partial \Phi_S^2} \right) = (\Delta\rho)^2 k_B T / I(0), \tag{19}$$

where $\Delta\rho$ is the scattering length density difference between the surfactant film and the two solvents.

The overall compositions of the samples investigated by SANS and the temperatures at which the experiments were performed are presented in Table II. We are particularly interested in the value of the extrapolated absolute scattered intensity at $q=0$. In the extrapolation process we have assumed that the scattered intensity at low q has a Lorentzian q dependence, the Ornstein-Zernike relation [28], also observed in sponge phases [16], resulting in a linear extrapolation of the inverse of the intensity versus q^2 as shown in the inset in Fig. 3. In Table III the experimental results are summarized. The second derivative of the free energy differs between the systems in a way that is qualitatively consistent with the observed difference in phase behavior. Due to the limited stability range of the balanced microemulsion phase it is not possible to solely form scattering data reliably to determine the functional form of how the free energy density depends on volume fraction. However, the data provide an absolute measure of the second derivative of the free energy.

VI. PHASE EQUILIBRIA

The chemical potentials are closely related to the first derivative of the free energy density. Thus by carefully determining phase boundaries we obtain data complementary to the values of the integral G/V obtained from surface tension data, and the second derivative, obtained from SANS measurements. We have confined the studies to systems with equal volume fraction of water and oil [29–31]. In Fig. 1 we illustrate the representation of the diagram, following a prin-

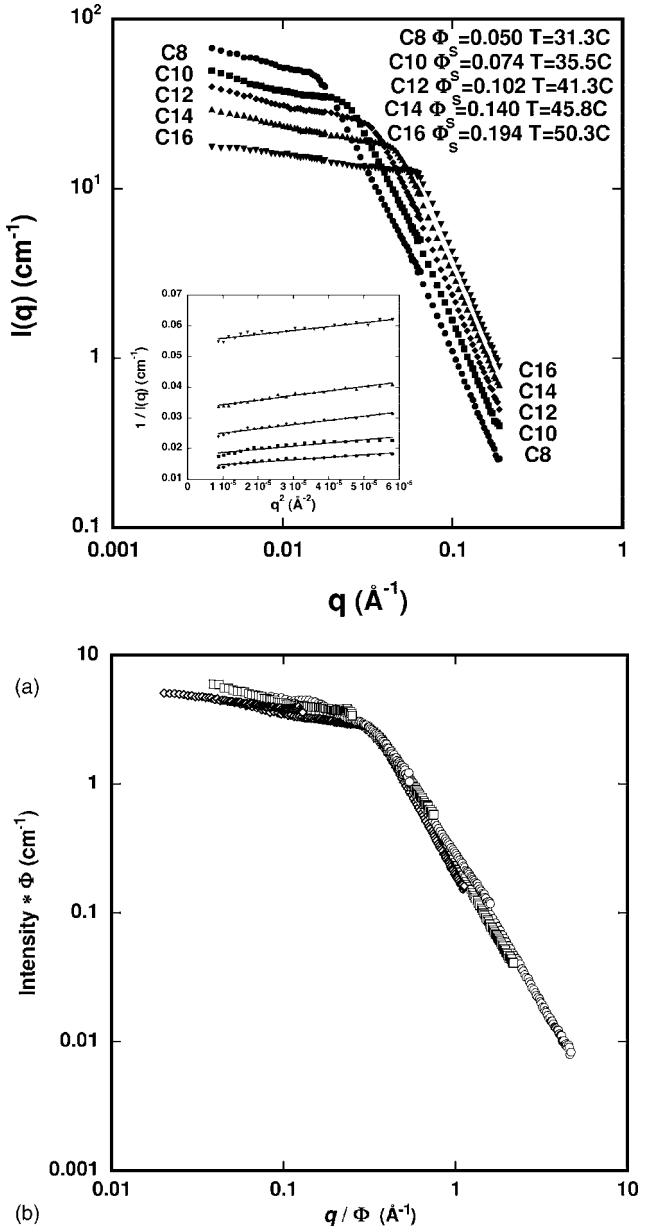

FIG. 3. The experimental scattering close to the balance temperature for the different oils are shown above with concentrations and temperatures written. (Volume fractions and temperatures are given for the samples.) The inset shows the inverse intensity versus the squared scattering length. This was used to get the intensity at zero scattering length. The symbols for the different oils are the same as in the big figure. The lines are fits. In (b) there is a way of "normalizing" the scattering for the different samples by multiplying the intensity with volume ratio and divide the scattering vector with volume ratio. Open circles are octane, open squares are dodecane, and open diamonds are hexadecane.

ciple developed by Kahlweit and coworkers, who have previously determined the equlibria relative to excess oil and water [4–7]. We reproduce these data, but have additionally used NMR and optical birefringence to establish also the two-phase area relative to the lamellar phase as illustrated in the Figs. 1 and 4. The equilibria at balanced conditions are of particular relevance for the analysis and the observed volume fractions are summarized in Table IV.

At balanced conditions the surfactant film does not to first order distinguish between the oil and the water and we can consider the system as a pseudo two-component one. Using this assumption the chemical potentials of the solvent, component 1, and surfactant, component 2, are obtained from G/V as

$$\mu_1/\nu_1 = \frac{G}{V} - \Phi_S \frac{\delta(G/V)}{\delta\Phi_S}, \tag{20a}$$

$$\mu_2/\nu_2 = \mu_1/\nu_1 + \frac{\delta(G/V)}{\delta\Phi_S}, \tag{20b}$$

where ν_i is the molecular volume of component i.

At maximum swelling $\Phi_S = \Phi_S^*$ of the microemulsion the solvent component is in equilibrium with pure water and oil implying that

$$\mu_1(\Phi_S{}^*) = 0, \tag{21}$$

which provides one condition on the for the derivative of G/V. The equilibrium microemulsion—lamellar phase provides additionally two

$$\mu_1(\Phi_{S1}) = \mu_1{}^{L\alpha}(\Phi_{S2}), \tag{22}$$

$$\mu_2(\Phi_{S1}) = \mu_2{}^{L\alpha}(\Phi_{S2}), \tag{23}$$

where Φ_{S1} and Φ_{S2} are volume fractions surfactant in the two coexisting phases respectively. A feature of these equations is that they remain unaffected when multiplying the free energy by a constant. However, if one relies on the free energy calculation by Helfrich for the lamellar phase as in Eq. (3) then the Eqs. (21)–(23) provide absolute relations for G/V for the microemulsion system.

The experimental data presented in Secs. III, V, and VI allows for both an evaluation of the parameters as well as a consistency test of the free energy expressions Eqs. (4) and (5). For each system we have six independent observations, except for hexadecane where the surface tension observation is missing. We now use these sets of data to separately analyze the two model free energy descriptions.

VII. FREE ENERGY AS A SERIES EXPANSION

In the final analysis of the free energy we will allow for only two terms in the expansion of Eq. (4). There is the generic third order term and a fifth order term that has to be positive to prevent the system to become infinitely stable at high concentrations. In principle there is also a fourth order term accounting for the asymmetry of the surfactant film in the higher order corrections. To reduce the number of parameters we assume that the coefficient of this term is small relative to the others, but one should be aware that using this approximation observed changes in the coefficients for the third and fifth order term might be due to changes in the suppressed fourth order term. Using Eqs. (4) and (20a) the condition Eq. (21) for maximum swelling of the microemulsion phase yields

TABLE II. Composition of the different samples where Φ_S is surfactant volume ratio of total sample volume, Φ_O is oil volume ratio of total oil and water for a mixture of deuterated and normal oil with the composition of deuterated oil in the last column and Φ_W is the deuterated water volume ratio of total oil and water. Here Φ_S is the total amount of surfactant and not the film forming surfactant.

Table II	Φ_S	$\Phi_O/(\Phi_O+\Phi_W)$	$\Phi_W/(\Phi_O+\Phi_W)$	% deuterated oil
Octane 1	0.0497	0.500	0.500	99.13
Octane 2	0.0579	0.504	0.496	99.13
Decane 1	0.0763	0.501	0.499	97.06
Decane 2	0.0805	0.504	0.496	97.06
Dodecane 1	0.0986	0.495	0.505	95.74
Dodecane 2	0.1102	0.503	0.497	95.74
Tetradecane 1	0.1377	0.496	0.504	94.82
Tetradecane 2	0.1477	0.503	0.497	94.82
Hexadecane 1	0.1827	0.499	0.501	94.60
Hexadecane 2	0.2017	0.498	0.502	94.60

$$-a_3 = 2a_5\Phi_S^{*2}. \tag{24}$$

Utilizing this relation and Eq. (3), the Eqs. (22) and (23) transform to

$$-a_3 = c_1T^2\lambda^3 \Bigg/ \left(\frac{\Phi_{S1}^2}{\Phi_S^{*2}} - 1\right) \tag{25}$$

and

$$-a_3 = 3c_1T^2\lambda^2\left\{\frac{5}{2}\left(\frac{\Phi_{S1}^2}{\Phi_S^{*2}}\right)^2 - 3 - 2\Phi_{S1}^2\left(\frac{\Phi_{S1}^2}{\Phi_S^{*2}} - 1\right)\right\}^{-1}. \tag{26}$$

Here $c_1 = 3\pi^2k_B^2/(128\kappa l_S^3)$ and $\lambda = \Phi_{S2}/[\Phi_{S1}(1-\Phi_{S2})]$. On the basis of these equations we can determine the coefficient a_3, a_5 by fitting to the experimental phase equilibrium data shown in Table IV. The Eqs. (25) and (26) provides two numerically independent estimates of the coefficient a_3. In Table V we summarize the fitted values for the five separate systems. The two different estimates of a_3 are clearly within the experimental uncertainty for all systems. Furthermore there is no major variation of the coefficient between the systems and it is our conclusion that within the accuracy of the analysis the value for a_3 is actually equal for all five systems. This is qualitatively consistent with the observation that the bending rigidities are also constant in the series. Below we will use the average value of $a_3 = 4.07 \times 10^5$ J in the analysis of the other parameters for all five systems. Thus the source of the difference in phase behavior is in the large variations in the higher order correction term a_5.

The SANS experiments provide a measure of the second derivative of the free energy density. In the series expansion model higher derivatives contains relatively seen larger contributions from the higher order terms. The SANS data thus provides a particularly critical test of this part of the free energy expression. Utilizing Eq. (24) we have

$$\frac{\delta^2G/V}{\delta\Phi_S^2} = -2a_3\Phi_S\left(\frac{5\Phi_S^2}{\Phi_S^{*2}} - 3\right). \tag{27}$$

From the comparison between calculated and experimental values for the second derivative, shown in Table V, we see that the estimated values are within experimental accuracy consistent with the experimental ones.

TABLE III. Composition of the different samples where Φ_S is surfactant volume ratio of film forming surfactant and the temperature of the measurement, T, and the difference from T_0. The fitted intensity at $q=0$ $I(0)$ and the calculated $\delta^2G/V/\delta\Phi_S^2$ from Eq. (19) for the two samples of each oil. Here we used $\Delta\rho = 6.2610^{10}$ cm^{-2}.

Table III	Octane	Decane	Dodecane	Tetradecane	Hexadecane
Φ_S	0.042	0.069	0.090	0.130	0.175
	0.050	0.074	0.102	0.140	0.194
$I(0)/\text{cm}^{-1}$	90.2	56.3	55.8	36.4	26.8
	71.6	54.9	42.0	30.3	18.3
T/K	304.3	308.6	314.4	318.9	323.4
T_0-T/K	0.1	0.9	0.75	0.4	0.1
$\delta^2G/V/\delta\Phi_S^2 10^{-5}$ Jm^{-3}	1.00	1.87	2.15	3.91	4.80
	2.08	2.51	3.69	5.31	7.38

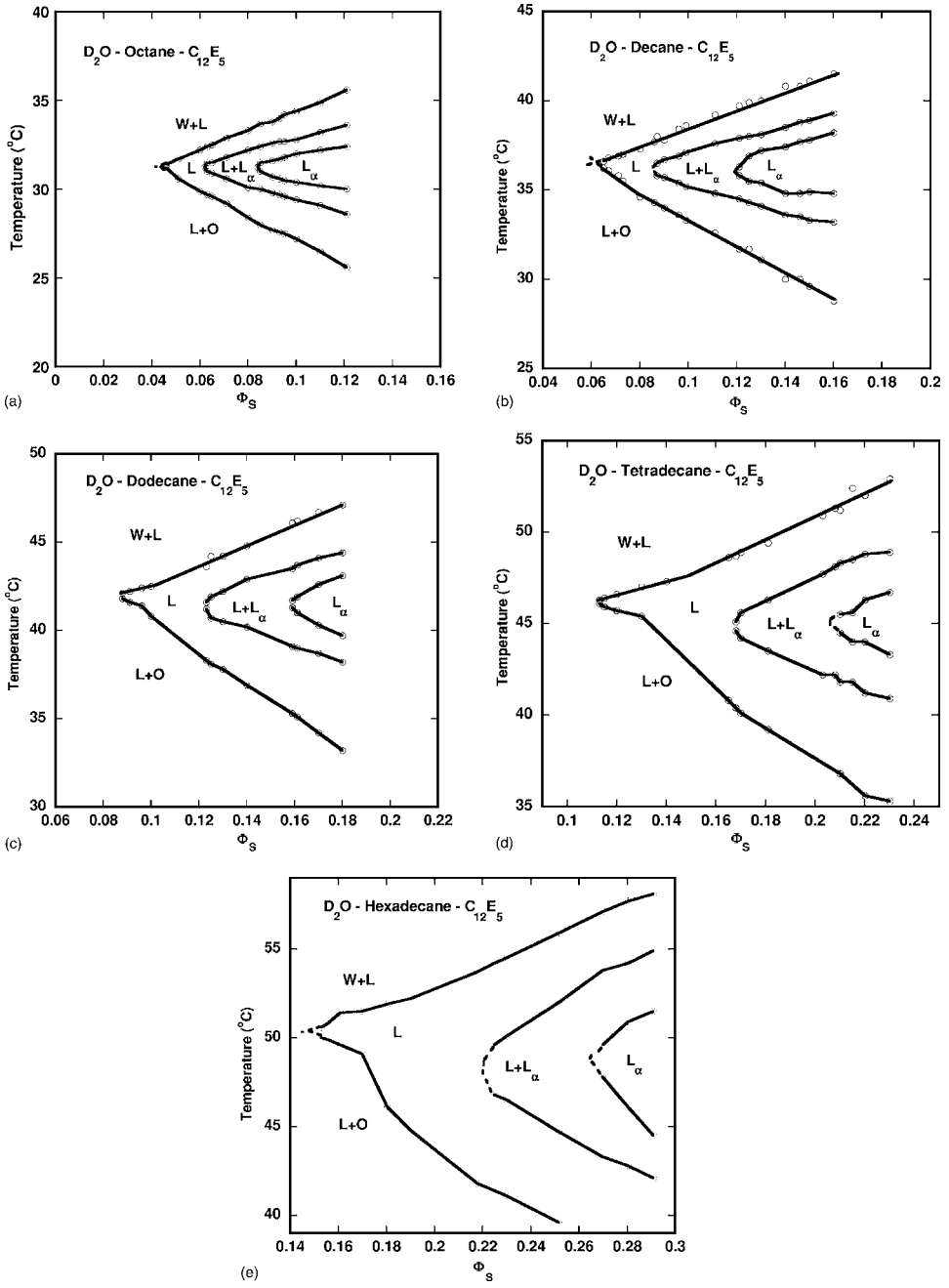

FIG. 4. (a–e) Phase diagram of the D_2O-oil-$C_{12}E_5$-system for a constant volume ratio oil-to-water 1:1. The phase diagram is shown as temperature versus the total volume ratio of surfactant. L denotes a liquid microemulsion phase, L_α is a lamellar liquid crystalline phase and $L+L_\alpha$ is the two-phase area in between. The volume fraction surfactant is the total volume fraction of surfactant as is standard for phase diagrams. The observed values of Φ_S^*, Φ_{S1}, and Φ_{S2} can then be recalculated with Eqs. (18a) and (18b) to be the volume fraction of the film forming surfactant. These recalculated values are used throughout the whole paper.

In Sec. II we concluded that the free energy density of the system at maximum swelling could be simply related to surface tension between water and oil in the three-phase triangle. Again utilizing Eq. (24) we have the simple relation

$$G/V(\Phi_S^*) = a_3\Phi_S^{*3}/2 \tag{28}$$

showing that the free energy at this point should vary as the third power of the concentration Φ_S^*. As seen in Table V the estimated values of $G/V(\Phi_S^*)$ are consistently somewhat smaller than the observed values. The agreement is satisfactory and it also shows that the measured values approximately follow the Φ_S^{*3} dependence.

The results shown in Table V shows that the free energy expansion of Eq. (4) with only a third and a fifth order term provides a good description of the observed properties. The relative variations between the five different systems are described very accurately and also the quantitative predictions are within the experimental uncertainties.

VIII. FREE ENERGY WITH LOGARITHMIC CORRECTION

The free energy density expression Eq. (5) contains the two parameters, a and b, in the free energy. To make the comparison as consistent as possible we adopt the same fitting procedure as in the previous section. The condition Eq. (21) of zero solvent chemical potential at maximum swelling of the microemulsion phase yields the relation

TABLE IV. The different volume ratios Φ_S^*, Φ_{S1}, and Φ_{S2}, being the finite swelling with a surfactant volume fraction, Φ_S^*, the maximum swelling with the surfactant volume fraction Φ_{S1} that coexists with the minimum lamellar with surfactant volume fraction Φ_{S2}. The temperature where the curvature was 0, T_0 is shown.

Table IV	Octane	Decane	Dodecane	Tetradecane	Hexadecane
Φ_S^*	0.036	0.057	0.077	0.104	0.144
Φ_{S1}	0.055	0.080	0.117	0.171	0.227
Φ_{S2}	0.085	0.114	0.153	0.213	0.269
T_0/K	304.4	309.5	315.1	319.3	323.5

$$b = -(\ln \Phi_S^* + 1/2)^{-1}. \tag{29}$$

The two Eqs. (22) and (23) specifying the equilibrium between microemulsion and lamellar phase transform to

$$a = c_1 T^2 \lambda^3 (1 + b \ln \Phi_{S1} + b/2)^{-1} \tag{30}$$

and

$$a = 3c_1 T^2 \lambda^3 \{(3 - 2\Phi_{S1})(1 + b \ln \Phi_{S1}) + b(1 - \Phi_{S1})\}^{-1}. \tag{31}$$

As summarized in Table VI the two independent estimates of the parameter a, assuming b to be given by Eq. (29), are reasonably consistent. However, the differences exceed 50% in one case. A further observation is that a as well as b and the product ab vary in a regular way in the homologous series of systems. The formal interpretation of the observed trend in the phase behavior is then that the decrease in maximum swelling with increasing alkyl chain length is due to an increase in the parameter b. The trend in the equilibrium with the lamellar phase is on the other hand due to the combined changes in a and b.

The second derivative of the free energy density obtained from the SANS data is

$$\frac{\delta^2 G/V}{\delta \Phi_S^2} = 6a\Phi_S(b \ln \Phi_S + 1 + 5b/6). \tag{32}$$

To obtain a quantitative prediction for this quantity we use for each system the average of the two values of a given in Table VI. Overall there is a good agreement between the predicted and the observed values.

For the free energy density at maximum swelling we find using Eq. (29)

$$G(\Phi_S^*) = a\Phi_S^{*3}(2 \ln \Phi_S^* + 1)^{-1}, \tag{33}$$

which for the relevant values of Φ_S^* implies a weaker than cubic dependence on Φ_S^*. This effect is seen in Table VI, where the agreement between calculated and observed values of $G/V(\Phi_S^*)$ improves for longer alkane systems. However there is a substantial discrepancy between calculated and experimental values for all system.

Combining the findings for the different observables the model free energy with a logarithmic correction term we find that it provides a consistently less good description of the system compared to the one derived from the series expansion. There is a substantial scatter between the two estimates of the coefficient a. For the integral free energy density the predicted values are off by more than a factor two.

IX. DISCUSSION

We have determined a number of different quantitative measures of the free energy of the microemulsion phase for the five different systems only differing by the nature of the oil. Changing this component has two effects on the phase behavior. First the balanced temperature T_0 increases by approximately 4 °C for each C_2H_4 that is added to the alkyl chain of the oil. This type of behavior [32,33] is commonly observed for microemulsions and it has been discussed in detail by Chen, Evans, and Ninham [34]. The effect has also been studied by Aveyard *et al.* [35] and by Meunier *et al.* [36]. The consensus interpretation is that an alkane with a

TABLE V. Summary of results using $a_3\Phi_S^3 + a_5\Phi_S^5$. Two independent values of a_3 are obtained from Eqs. (25) and (26), respectively. Here $c_1 = 3\pi^2 k_B^2/(128\kappa l_S^3)$ with $\kappa = 1.0 \times 10^{-20}$ and $l_S = 15$ Å which gives $c_1 = 1.30$. The average $a_3 = -4.07 \times 10^5 J/m^3$ is used for calculation of a_5. The numbers in brackets are the experimental values.

Table V	Octane	Decane	Dodecane	Tetradecane	Hexadecane
$-a_3(\mu_i) \times 10^{-5}$ Jm^{-3}	4.29	5.33	3.63	3.08	3.90
	3.84	5.46	3.77	3.13	4.23
$a_5 \times 10^{-7}$ Jm^{-3}	15.6	6.24	3.35	1.89	0.98
$G/V(\Phi_S^*)$ Jm^{-3}	−9.1 (−12.1)	−38 (−34.2)	−92 (−119)	−228 (−325)	−605
$\delta^2 G/V/\delta\Phi_S^2 10^{-5}$ Jm^{-3}	1.30 (1.83)	2.43 (2.96)	2.80 (3.05)	5.08 (4.74)	6.24 (6.53)
	2.70 (2.30)	3.26 (3.04)	4.80 (4.05)	6.90 (5.69)	9.59 (9.59)

TABLE VI. Summary of the results using $a_3\Phi_S^3(1-b\ln\Phi_S)$. Here $c_1=3\pi^2k_B^2/(128\kappa l_S^3)$ with $\kappa=1.0\times10^{-20}$ and $l_S=15$ Å which gives $c_1=1.30$. The numbers in brackets are the experimental values.

Table VI	Octane	Decane	Dodecane	Tetradecane	Hexadecane
$a(\mu_i)\times10^{-5}$ Jm^{-3}	38.6	41.5	23.5	18.6	16.0
	40.2	69.7	30.3	21.3	16.3
a average	39.4	55.6	26.9	20.0	16.2
b	0.354	0.432	0.485	0.567	0.628
$G/V/(\Phi_S^*)$ Jm^{-3}	−33 (−12.1)	−218 (−34.2)	−298 (−119)	−638 (−325)	−1673
$\delta^2G/V/\delta\Phi_S^2\times10^{-5}$ Jm^{-3}	1.72 (1.83)	4.72 (2.96)	3.43 (3.05)	4.93 (4.74)	7.25 (6.53)
	2.77 (2.30)	5.81 (3.04)	4.89 (4.05)	6.02 (5.69)	9.26 (9.59)

shorter chain more readily penetrates the alkyl chain layer of the surfactant film. At a given temperature exchanging octane for decane would give less penetration moving the spontaneous curvature to more positive values. For ethylene oxide surfactants the original spontaneous curvature can then be restored by increasing the temperature. The second effect of extending the alkyl chain length is to move phase boundaries to higher volume fractions of the surfactant. This is the effect on which this paper is focused. Exchanging the oil is a minor perturbation on the system and yet there are major quantitative changes in the phase behavior.

We have tested two model free energy expressions relative to the experimental free energy data. Both expressions contain two free parameters that where fitted to the phase equilibrium data. For the power series expansion we find that the expression provides a consistent description of the phase data. It is a significant observation that within the experimental accuracy this coefficient is the same for all five systems. One can note that the determination of the absolute magnitude of coefficients a_3, a_5, and a relies on an assumed correctness of Helfrich's expression for the undulation force and a correct value for the bending rigidity, κ. A change of the numerical value of the coefficient c_1 gives a proportional change in the estimated value for the parameters.

The free energy expression based on the renormalization model with a logarithmic correction term describes the data less well. Overall the model shows minor inconsistencies and some clear discrepancies when tested against the experimental data. However, these difficulties could possibly be attributed to experimental inaccuracies.

Another aspect of the problem is obtained when considering the physical origin of the terms in the free energy. Based on the Porte scaling concept we see two different contributions to the generic a_3 (or a) Φ_S^3 term. Using the Gauss-Bonet theorem it follows that there is a bending free energy for forming the topologically complex bicontinuous structure of the microemulsion. This contribution amounts to

$$a_3(\bar{\kappa}) = -2\bar{\kappa}/l_S^3. \tag{34}$$

Since $\bar{\kappa}$ is expected to be negative it gives a positive contribution to forming the microemulsion. The microemulsion consists of a disordered surfactant film that extends in three dimensions. There is an entropy associated with this disorder and this provides an opposing negative contribution to a_3. For a given topology of the film the magnitude of this entropic term is determined by κ. The result in the series expansion model, that a_3 takes a negative sign, then signals that the entropic contribution dominates over the $\bar{\kappa}$ term. This observation is consistent with our previous observation [16] that for a sponge phase containing the same components the $\bar{\kappa}$ term slightly dominates over the entropy term. In this case both κ and $\bar{\kappa}$ are approximately twice as large since one is dealing with a bilayer. We consider it a problem for the series expansion model that based on our previous uncertain estimate of $\bar{\kappa}\approx8\times10^{-21}$ the estimated contribution to a_3 according to Eq. (34) is around 5×10^6 J/m^3, which is 16 times larger in magnitude than the estimated value of a_3. This would imply near cancellation between the entropic and topology contributions to a_3. A smaller magnitude of $\bar{\kappa}$ would provide a more consistent picture.

For the free energy based on the renormalization mechanism the a term is large and positive. For octane the fitted value of 4×10^6 J/m^3 is only a little smaller than the $\bar{\kappa}$ contribution using the value of $\bar{\kappa}\approx-8\times10^{-21}$ J. The entropic contribution to a is then smaller in magnitude. Problems arise when we transform such a result to a description of the sponge phase, where the values of the elastic constants are roughly twice as large. For such a phase the saddle splay bending term, $\bar{\kappa}$, would then completely dominate over the entropic contribution. It is difficult to reconcile this result with the observed stability range for the sponge phase.

In this paper we have demonstrated a procedure for obtaining different quantitative measures of the free energy of a balanced microemulsion. The experimental results have been used to test two previously suggested functional forms of the free energy density. We find that a series expansion containing a third and a fifth order term provides a good description of the data. For the expression containing a logarithmic correction term there are clear difficulties in accounting for the observations, but the discrepancies are not of such a major character that we can convincingly conclude that the description is invalid.

ACKNOWLEDGMENTS

This work was financially supported by the Swedish Foundation for Strategic Research (SSF) through the Colloid and Interface Technology Programme. U.O and H.W thank

the Swedish Research Council (V.R.) for financial support. H.K thanks the DAAD for funding. This work is based on experiments performed at the Swiss spallation neutron source SINQ, Paul Scherrer Institute, Villingen, Switzerland. This research project has been supported by European Commission under the 6th Framework Programme through the Key Action: Strengthening the European Research Area, Research Infrastructures. Contract No. RII-CT-2003-505925. We are grateful for the help from Joachim Kohlenbrecher and Steven van Petegem during our stay at PSI.

[1] D. F. Evans and H. Wennerström, *The Colloidal Domain: Where Physics, Chemistry, Biology and Technology Meet* (John Wiley & Sons, Inc, New York, 1999).
[2] P. Kumar and K. L. Mittal (Marcel Dekker, New York, 1999), p. 849.
[3] K. Holmberg, *Handbook of Applied Surface and Colloid Chemistry Volume 1* (John Wiley & Sons Ltd, Chichester, 2002).
[4] T. Sottmann, R. Strey, and S. H. Chen, J. Chem. Phys. **106**, 6483 (1997).
[5] T. Sottmann and R. Strey, J. Chem. Phys. **106**, 8606 (1997).
[6] M. Kahlweit, R. Strey, P. Firman, D. Haase, J. Jen, and R. Schomacker, Langmuir **4**, 499 (1988).
[7] F. Lichterfeld, T. Schmeling, and R. Strey, J. Phys. Chem. **90**, 5762 (1986).
[8] H. Wennerström and U. Olsson, Langmuir **9**, 365 (1993).
[9] S. A. Safran, in *Structures and Dynamics of Strongly Interacting Colloids and Supramolecular Aggregates in Solution*, edited by S. Chen, J. S. Huang, and P. Tartaglia (Kluwer Academic Publishers, Dordrecht, The Netherlands, 1992).
[10] J. Daicic, U. Olsson, and H. Wennerström, Langmuir **11**, 2451 (1995).
[11] W. Helfrich, Z. Naturforsch. A **28c**, 693 (1973).
[12] G. Porte, J. Appell, P. Bassereau, and J. Marignan, J. Phys. (Paris) **50**, 1335 (1989).
[13] W. Helfrich, Z. Naturforsch. A **33a**, 305 (1978).
[14] W. Helfrich, J. Phys.: Condens. Matter **6**, A79 (1994).
[15] J. Daicic, U. Olsson, H. Wennerström, G. Jerke, and P. Schurtenberger, J. Phys. I **5**, 199 (1995).
[16] T. D. Le, U. Olsson, H. Wennerström, and P. Schurtenberger, Phys. Rev. E **60**, 4300 (1999).
[17] S. A. Safran, D. Roux, M. E. Cates, and D. Andelman, Phys. Rev. Lett. **57**, 491 (1986).
[18] D. Andelman, M. E. Cates, D. Roux, and S. A. Safran, J. Chem. Phys. **87**, 7229 (1987).
[19] M. E. Cates, D. Andelman, S. A. Safran, and D. Roux, Langmuir **4**, 802 (1988).
[20] G. Gompper, D. Richter, and R. Strey, J. Phys.: Condens. Matter **13**, 9055 (2001).
[21] T. Hellweg and D. Langevin, Phys. Rev. E **57**, 6825 (1998).
[22] T. Hellweg and D. Langevin, Physica A **264**, 370 (1999).
[23] A. Evilevitch, U. Olsson, B. Jönsson, and H. Wennerström, Langmuir **16**, 8755 (2000).
[24] A. Abragam, *Principles of Nuclear Magnetism* (Clarendon Press, Oxford, 1961).
[25] J. Kohlbrecher and W. Wagner, J. Appl. Crystallogr. **33**, 804 (2000).
[26] U. Keiderling, Appl. Phys. A: Mater. Sci. Process. **74**, s1455 (2002).
[27] S. Burauer, T. Sachert, T. Sottmann, and R. Strey, Phys. Chem. Chem. Phys. **1**, 4299 (1999).
[28] L. S. Ornstein and F. Zernike, Proc. K. Ned. Akad. Wet. **17**, 793 (1914).
[29] M. Kahlweit and R. Strey, Angew. Chem., Int. Ed. Engl. **24**, 654 (1985).
[30] M. Kahlweit, R. Strey, and P. Firman, J. Phys. Chem. **90**, 671 (1986).
[31] T. Sottmann and R. Strey, J. Phys.: Condens. Matter **8**, A39 (1996).
[32] D. W. R. Gruen, Biochim. Biophys. Acta **595**, 161 (1980).
[33] D. W. R. Gruen and D. A. Haydon, Biophys. J. **33**, 167 (1981).
[34] S. J. Chen, D. F. Evans, and B. W. Ninham, J. Chem. Phys. **88**, 1631 (1984).
[35] R. Aveyard, P. Cooper, and P. D. I. Fletcher, J. Chem. Soc., Faraday Trans. **86**, 3623 (1990).
[36] H. Kellay, Y. Hendrikx, J. Meunier, B. P. Binks, and L. T. Lee, J. Phys. I **3**, 1747 (1993).